Available online at www.sciencedirect.com

ScienceDirect

IFAC PapersOnLine 56-2 (2023) 10396–10401

A robust optimization approach for dynamic input allocation ⋆

Alessandro Tenaglia * Federico Oliva * Mario Sassano * Sergio Galeani * Daniele Carnevale *

* Department of Civil Engineering and Computer Science Engineering, University of Rome Tor Vergata, Rome, Italy (e-mail: {alessandro.tenaglia, federico.oliva, mario.sassano, sergio.galeani, daniele.carnevale}@uniroma2.it

Abstract: This paper addresses the problem of dynamic input allocation in the presence of plant uncertainties. The current state of the art shows how to design an *Allocator* as the cascade of an *Optimizer* and an *Annihilator* to achieve steady-state input optimality and output invisibility simultaneously. This work proposes a novel algorithm based on polynomial factorization to design a dynamic *Annihilator*. The critical aspect of this approach lies in the assumption of the perfect plant knowledge, making the *Annihilator* not robust to uncertainties. A robustification process is introduced by optimizing its design parameters. This approach is formulated as a model-matching problem aiming to reduce the output mismatch induced by the allocation scheme while maintaining steady-state optimality. As the numerical simulations highlight, this method applies to linear and nonlinear allocation problems.

Keywords: Robust control applications, Uncertain systems, Input allocation, Parametric optimization, Systems with saturation.

1. INTRODUCTION

When designing suitable control laws for a system, the structure and the number of actuators play a crucial role in the synthesis problem. Actuators can be selected depending on power-related assumptions to increase robustness through redundancy or to reach specific performance (e.g., Hamandi et al. (2021)). Input allocation represents a field of Control Theory that builds on top of a predetermined control law and exploits input redundancy of the plant to maximize the actuator's performance without affecting the system output; such a condition is usually defined as *output invisibility*. The actuator's performance is evaluated through a specific cost, e.g., total power consumption, distance from saturation limits, or fast zero-crossing. For a general review of the topic, the reader may refer to Zaccarian (2009), and Johansen and Fossen (2013). The set of potential applications is quite vast. For example, Trégouët et al. (2014) uses a static input allocation scheme for reaction wheels desaturation on low-orbit satellites. Instead, Furci et al. (2019) uses similar results to implement a hierarchical control architecture in an over-actuated hovercraft-like system. In particular, the allocation scheme also handles nonlinearities in the model. Fault Tolerance Control applications based on input allocation are also proposed by Argha et al. (2019). Lastly, it is essential to remark that input allocation has been widely used in Nuclear Fusion research, specifically in Tokamaks, exploiting the reactor coil redundancy to control plasma position and elongation safely. Refer to Boncagni et al. (2011); Ambrosino et al. (2011); Esposito et al. (2016) for more information. Input allocation was first developed on LTI systems, where the *input redundancy* property can be easily defined (Zaccarian (2009)). Indeed, an LTI system can be non-, weakly, or strongly redundant. As discussed in Galeani and Pettinari (2014), and Cristofaro and Galeani (2014), the *Allocator* can be designed as the cascade of a steady-state *Optimizer* and an *Annihilator*. Using a static *Annihilator*, the difference between weak and strong redundancy is that in the former, output invisibility is ensured only at steady-state, while in the latter, at any time. Output invisibility can also be achieved for weakly redundant systems using a dynamic *Annihilator* as discussed in Cristofaro and Galeani (2014). Additional allocation techniques have been introduced in Galeani et al. (2015) and Galeani and Sassano (2018b) to handle the output-regulation problem on linear over-actuated systems. The knowledge of the nominal plant is often quite accurate at low frequencies rather than at higher ones due to nonlinearities and time-varying effects. The potential problem is that *Allocator* is designed on the nominal plant. Thus, model uncertainties result in the loss of the output invisibility property.

The main contribution of this paper is the design of a dynamic allocation scheme that ensures robustness in determining model uncertainties. A data-driven approach to solve a similar problem has been introduced by Galeani and Sassano (2018a). Instead, the proposed method relies on optimization techniques where the output invisibility is cast as a model-matching problem, and the model mismatch is considered in the minimization goal.

⋆ This work has been partially supported by the Italian Ministry for Research in the framework of the 2020 Program for Research Projects of National Interest, Grant No. 2020RTWES4, and by EUROfusion Consortium, Grant No. 101052200.

10.1016/j.ifacol.2023.10.1053

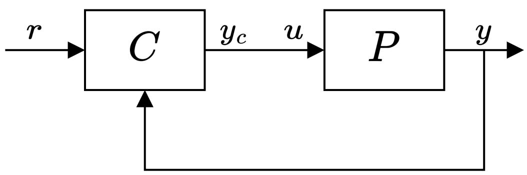

Fig. 1. The original closed-loop system Σ.

Novel contribution. The main novelties proposed in this paper consist of the following:

- showing how a robust input *Allocator* allows to improve performances in the presence of plant uncertainties;
- providing an algorithm to design an *Annihilator*;
- providing an algorithm to robustify an *Allocator*;
- raising the issue of designing a robust input *Allocator*. In fact, to the best of the authors' knowledge, no robust allocation techniques have been proposed yet.

The rest of the paper is organized as follows. Section 2 describes the problems of interest. In Section 3, input allocation schemes are recalled, and a new algorithm is proposed for the *Allocator* design. Section 4 defines the robust allocation procedure with the proposed optimization-based solution. Lastly, Section 5 shows extensive numerical results supporting the validity of the approach proposed in Section 4, while Section 6 draws conclusions and future research directions.

2. PROBLEM STATEMENT

Consider a finite set of Linear Time-Invariant (LTI) systems $\mathcal{P}$ with cardinality $|\mathcal{P}| = N$, where the trajectories of each plant $P \in \mathcal{P}$ can be described as the output of the standard state-space formulation

$$\dot{x} = Ax + Bu, \tag{1a}$$
$$y = Cx + Du, \tag{1b}$$

where $x \in \mathbb{R}^n$ is the plant state, $u \in \mathbb{R}^m$ is the plant input, and $y \in \mathbb{R}^p$ is the plant output. We also assume that the plant considered is *fat*, namely $m > p$. In the analysis carried out in this work, one of the plants in $\mathcal{P}$ is considered the nominal one P_0, and referred to as

$$\dot{x} = A_0 x + B_0 u, \tag{2a}$$
$$y = C_0 x + D_0 u. \tag{2b}$$

Moreover, it is assumed that a robust controller C for the set $\mathcal{P}$ in (1) is available, given by

$$\dot{x}_c = A_c x_c + B_c u_c + B_r r, \tag{3a}$$
$$y_c = C_c x_c + D_c u_c + D_r r, \tag{3b}$$

where $x_c \in \mathbb{R}^{n_c}$ is the controller state, $u_c \in \mathbb{R}^p$ is the controller input, $r \in \mathbb{R}^p$ is a constant reference signal and $y_c \in \mathbb{R}^m$ is the controller output. As far as stability is concerned, the following assumption is considered valid throughout the paper.

Assumption 1. The closed-loop system Σ in Fig. 1 given by (1) and (3), with $u_c = y$ and $u = y_c$, is well-posed and asymptotically stable, for each $P \in \mathcal{P}$.

The standard allocation problem consists of designing an *Allocator* described as

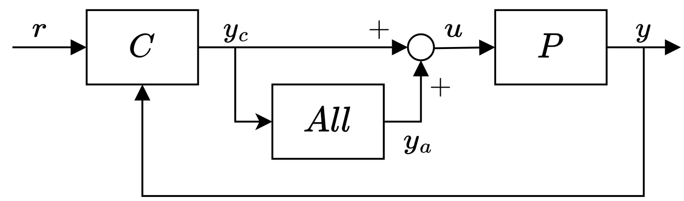

Fig. 2. The allocated closed-loop system Σ_{all}.

$$\dot{x}_a = f_a(x_a, u_a), \tag{4a}$$
$$y_a = g_a(x_a, u_a), \tag{4b}$$

where $x_a \in \mathbb{R}^{n_a}$ is the allocator state, $u_a \in \mathbb{R}^m$ is the allocator input, and $y_a \in \mathbb{R}^m$ is the allocator output, which is connected to (1) and (3), as shown in Fig. 2, according to the following

$$u_a = y_c, \tag{5a}$$
$$u = y_c + y_a. \tag{5b}$$

This system exploits the input redundancy of P to modify the plant input u, optimizing a specific cost function without altering the plant output y (Galeani and Pettinari (2014)). In summary, the following general problem can be defined.

Problem 1. (Nominal input allocation). Consider the nominal closed-loop system Σ_0, namely $\mathcal{P} = \{P_0\}$, and design, if possible, an input *Allocator* such that the allocated closed-loop system $\Sigma_{0,all}$ given by (2), (3), (4) and (5):

- **(AS)** is well-posed and asymptotically stable;
- **(I)** ensures output invisibility, namely, with the same initial condition of P_0, C and reference signal, the output y of Σ_0 and the output y_{all} of $\Sigma_{0,all}$ coincide;
- **(O)** ensures steady-state optimality, namely the steady-state plant input $u_\infty = y_{c,\infty} + y_{a,\infty}$ satisfies:

$$J(u_\infty) = \min_{v \in U_{\Sigma_0}} J(v), \tag{6}$$

where J is a cost function with domain on $\mathbb{R}^m$ and U_{Σ_0} is the set of all admissible inputs v for the closed-loop system Σ_0.

In the case of no uncertainties, namely $\mathcal{P} = \{P_0\}$, then an *Allocator* solving Problem 1 can be designed, e.g., as shown in Galeani and Pettinari (2014), and Cristofaro and Galeani (2014). However, when plant uncertainties are considered, namely $|\mathcal{P}| = N > 1$, the *Allocator* designed only on P_0 no longer ensures output invisibility (I) for each $P \in \mathcal{P}$. Hence, in this paper, we propose a design procedure for a robust *Allocator*, redefining Problem 1 as follows.

Problem 2. (Robust input allocation). Consider the closed-loop system Σ and design, if possible, an input *Allocator* such that for each $P \in \mathcal{P}$ the allocated closed-loop system Σ_{all} given by (1), (3), (4) and (5):

- **(AS)** is well-posed and asymptotically stable;
- **(NI)** ensures output invisibility in the nominal case, i.e., item (I) of Problem 1;
- **(NO)** ensures steady-state optimality in the nominal case, i.e., item (O) of Problem 1;
- **(RIO)** minimizes the cost function

$$\tilde{J}(\Theta) = \sum_{i=1}^{N} \left(\int_0^T \|\delta y_i\|^2 + \alpha J(u_{all,i}(t)) \mathrm{d}t \right), \tag{7}$$

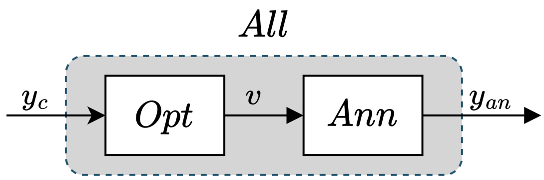

Fig. 3. The internal structure of the *Allocator*: a cascade of a steady-state *Optimizer* and an *Annihilator*.

with respect to the *Allocator*'s set of design parameters Θ, defined in Section 3. In (7), T is the time horizon considered, the subscript i refers to the trajectories related to a $P_i \in \mathcal{P}$, $\delta y_i(t) = y_{all,i}(t) - y_i(t)$ is the output mismatch between the closed-loop Σ_i and the corresponding allocated closed-loop $\Sigma_{all,i}$, with the same initial condition of P_i, C and reference signal. Furthermore, $u_{all,i}$ is the plant allocated input, J is the cost function defining optimality in allocation design, i.e., item (O) of Problem 1, and $\alpha > 0$ is a scaling factor. Equation (7) represents a suitable cost function because it depends on the output mismatch δy_i and on (6).

3. ALLOCATOR DESIGN

We first proceed by designing an *Allocator* solving Problem 1. Cristofaro and Galeani (2014), and Galeani and Pettinari (2014) show that such an *Allocator* does exist and has a general architecture represented by a cascade of two systems, namely a steady-state *Optimizer* and an *Annihilator*, as shown in Fig. 3. The *Optimizer* aims to satisfy item (O) of Problem 1, while the *Annihilator* deals with item (I). Thus, the design of the *Allocator* can be performed in two steps: first, the design of the *Annihilator* and then the design of the steady-state *Optimizer*.

3.1 Annihilator Design

In the literature, several algorithms have been proposed to design an *Annihilator*; for example, Cristofaro and Galeani (2014) uses the Smith form of the plant numerator, while Galeani and Sassano (2018a) exploits the orthogonal moments of the plant. In this work, we propose a novel and straightforward approach based on polynomial factorization, providing a numerical procedure for the design of an *Annihilator* starting from the state-space representation of (2). The *Annihilator* is given by

$$\dot{x}_{an} = A_{an} x_{an} + B_{an} v, \tag{8a}$$
$$y_{an} = C_{an} x_{an}, \tag{8b}$$

where $x_{an} \in \mathbb{R}^{n_{an}}$ is the annihilator state, $v \in \mathbb{R}^{\eta}$ is the optimizer output, $y_{an} \in \mathbb{R}^m$ is the annihilator output. We refer to $W_{an}(s)$ as the transfer function from v to y_{an}. Thus, denoting with

$$W_0(s) = C_0(sI - A_0)^{-1}B_0 + D_0 \tag{9}$$

the transfer function from u to y of P_0 in (2), the item (I) of Problem 1 is satisfied if

$$W_0(s)\, W_{an}(s) = 0. \tag{10}$$

Again, the *Annihilator* design aims to define $W_{an}(s)$ to ensure output invisibility with respect to P_0. The first step of the algorithm consists of computing a left polynomial factorization of (9)

$$W_0(s) = D^{-1}(s)N(s), \tag{11}$$

where $D(s)$ is a square nonsingular polynomial matrix, i.e., such that $\det(D(s))$ is not identically zero, and $N(s)$ is a polynomial matrix as well, described by

$$N(s) = N_n s^n + N_{n-1}s^{n-1} + ... + N_1 s + N_0, \tag{12}$$

with $N_i \in \mathbb{R}^{p\times m}$.

Now, the $(sI - A_0)^{-1}$ term in (9) can be computed using the adjoint method, namely

$$(sI - A_0)^{-1} = \frac{1}{\det(sI - A_0)} \operatorname{adj}(sI - A_0). \tag{13}$$

where $\det(sI - A_0)$ and $\operatorname{adj}(sI - A_0)$ are the determinant and the adjoint matrix of $sI - A_0$, respectively, described by

$$\det(sI - A_0) \triangleq s^n + a_{n-1}s^{n-1} + ... + a_1 s + a_0, \tag{14a}$$
$$\operatorname{adj}(sI - A_0) \triangleq E_{n-1}s^{n-1} + ... + E_1 s + E_0. \tag{14b}$$

with $a_i \in \mathbb{R}$ and $E_i \in \mathbb{R}^{n\times n}$. Substituting (13) and (14) in (11), the following relations are obtained

$$D(s) = \sum_{k=0}^{n} a_k s^k I, \tag{15a}$$
$$N(s) = \sum_{k=0}^{n} (C_0 E_k B_0 + a_k D_0)s^k. \tag{15b}$$

The set of a_k and E_k in (14) is computed using the *Souriau-Leverrier-Faddeev* algorithm (Faddeev and Faddeeva (1981)), which we report here for completeness. Define $a_n \triangleq 1$, $E_n \triangleq 0_n$ and $E_{-1} \triangleq 0_n$. The remaining set of a_i and E_i are computed recursively with

$$E_{n-k} = a_{n-k+1} I_n + A_0 E_{n-k+1}, \quad k = 1, \dots n+1, \tag{16a}$$
$$a_{n-k} = -\frac{1}{k} \operatorname{tr}(A_0 E_{n-k}), \quad k = 1, \dots n, \tag{16b}$$

where $\operatorname{tr}(\cdot)$ is the trace operator.

The second step of the algorithm is to compute the *Annihilator* transfer function $W_{an}(s)$ satisfying (10), which is represented by a right polynomial factorization, namely

$$W_{an}(s) = N^{\perp}(s)\Psi^{-1}(s) \tag{17}$$

where $\Psi(s)$ is a square and nonsingular polynomial matrix, i.e., such that $\det(\Psi(s))$ is not identically zero, and $N^{\perp}(s)$ is a polynomial matrix as well, described by

$$N^{\perp}(s) = N^{\perp}_{\eta} s^{\eta} + N^{\perp}_{\eta-1}s^{\eta-1} + ... + N^{\perp}_1 s + N^{\perp}_0, \tag{18}$$

with $N^{\perp}_i \in \mathbb{R}^{m\times m-p}$ and where we select $\eta = n$. To meet (10), the following necessary and sufficient conditions must be met,

$$N(s)N^{\perp}(s) = 0, \tag{19}$$

namely $N^{\perp}(s)$ needs to be a polynomial basis for the null space of the polynomial matrix $N(s)$. By substituting (12) and (18) in (19), we obtain the following

$$(N_n s^n + ... + N_0)(N^{\perp}_{\eta} s^{\eta} + ... + N^{\perp}_0) = 0. \tag{20}$$

By expanding the polynomial product and rearranging the terms in a matrix form, (20) can be written as the product of a band matrix $\bar{N}$ and a matrix $\bar{N}^{\perp}$. $\bar{N}$ is built up by the coefficient matrices of $N(s)$, while $\bar{N}^{\perp}$ is obtained by stacking the coefficient matrices of $N^{\perp}(s)$:

$$\begin{bmatrix} N_0 & 0 & \dots & 0 \\ N_1 & N_0 & \dots & 0 \\ \vdots & \vdots & \ddots & \vdots \\ N_n & N_{n-1} & \cdots & N_0 \\ \vdots & \ddots & \vdots & \vdots \\ 0 & \dots & N_n & N_{n-1} \\ 0 & \dots & 0 & N_n \end{bmatrix} \begin{bmatrix} N_0^{\perp} \\ N_1^{\perp} \\ \\ \vdots \\ N_{\eta-1}^{\perp} \\ N_{\eta}^{\perp} \end{bmatrix} = \bar{N}\bar{N}^{\perp} = 0. \qquad (21)$$

In this way, the *Annihilator* numerator can be obtained simply by computing the null space of a band matrix and choosing $m-p$ vectors in the basis found.

The final step of the algorithm is to define the invertible polynomial matrix $\Psi(s)$ in (17) to have a stable and realizable $W_{an}(s)$. This can be achieved by simply choosing $\Psi(s) = \boldsymbol{\psi}(s)I_{m-p}$, where I_{m-p} is the identity matrix of order $m-p$ and $\boldsymbol{\psi}(s)$ any Hurwitz polynomial with $\deg(\boldsymbol{\psi}(s)) > \eta$. Therefore, the choice of denominator represents a degree of freedom that can be used to achieve better performance for the *Allocator*; this aspect will be further investigated in Section 4. In summary, an *Annihilator* can be designed following the subsequent algorithm.

Algorithm 1. **Annihilator design**

- Compute a left polynomial factorization $D^{-1}(s)N(s)$ of (9) using (15) and (16).
- Compute the null space of $\bar{N}$ in (21) and define $N^{\perp}(s)$ rearranging the solution in a polynomial form as in (18).
- Choose a Hurwitz polynomial $\boldsymbol{\psi}(s)$ with $\deg(\boldsymbol{\psi}(s)) > \eta$, and define $\Psi(s) = \boldsymbol{\psi}(s)I_{m-p}$.
- Define the *Annihilator* for (1) as any minimal realization of $W_{an}(s) = N^{\perp}(s)\Psi^{-1}(s)$.

3.2 Optimizer Design

The overall *Allocator* design is completed by selecting a suitable steady-state *Optimizer*, in line with Fig. 3, as shown in Galeani and Pettinari (2014). Remembering that the goal of the *Optimizer* is to achieve item (O) of Problem 1, a gradient law on the desired cost function $J(u_\infty)$ can be used, so the *Optimizer* is defined by

$$\dot{x}_{op} = -\Gamma \nabla J(y_c + \Omega_{an} x_{op}), \qquad (22a)$$

$$v = x_{op}, \qquad (22b)$$

where $x_{op} \in \mathbb{R}^{m-p}$ is the optimizer state, $v \in \mathbb{R}^{m-p}$ is the optimizer output, and $\Omega_{an} = W_{an}(0)$. Lastly, $\Gamma \in \mathbb{R}^{m-p\times m-p}$, $\Gamma > 0$ is a suitable matrix that regulates the convergence rate. Γ is an additional degree of freedom that can be exploited in the construction of the *Allocator*, which is considered in the Section 4.

4. ROBUST ALLOCATOR DESIGN

The *Allocator* design described in Section 3 successfully solves Problem 1. However, this work aims to solve the robust input allocation problem, i.e., Problem 2. Indeed, the procedure described in Section 3 provides an *Allocator* structurally designed to obtain output invisibility on P_0. However, if that *Allocator* is implemented on any $P \in \mathcal{P}$, in general, the output invisibility property is lost; namely, a mismatch exists between the original and the allocated outputs.

The core idea is to formulate Problem 2 as a model-matching problem (MMP) between the non-allocated and allocated closed-loop systems, finding an opportune selection of the *Allocator* parameters introduced in Section 3 to achieve item (RIO). A possible way to solve such a problem would use the design parameters to define a static state-feedback for the *Allocator*. On top of this, several goals could be addressed, such as an H_∞ MMP, which can be solved using the linear matrix inequality (LMI) optimization, but limiting its applicability to linear systems only.

The method proposed defines an optimization-based procedure to robustify a dynamic allocation scheme concerning plant uncertainties. From Section 3, the *Annihilator* denominator $\boldsymbol{\psi}(s)$ and the *Optimizer* gain matrix Γ can be considered as design parameters of the *Allocator*. Therefore, we define the following minimization problem to achieve item (RIO) of Problem 2:

$$\begin{aligned} \min_{\Gamma,\boldsymbol{\psi}} \quad & \sum_{i=1}^{N} \left(\int_0^T \|\delta y_i\|^2 + \alpha J(u_{all,i}(t)) \mathrm{d}t \right) \\ \text{s.t.} \quad & \Gamma = \mathrm{diag}(\gamma_1, \dots \gamma_{m-p}) > 0, \\ & \boldsymbol{\psi}(s) \text{ is Hurwitz with } \deg(\boldsymbol{\psi}(s)) = \eta + 1. \end{aligned} \qquad (23)$$

$\boldsymbol{\psi}(s)$ and Γ are constrained to have a specific structure. First, the gain matrix Γ is assumed to be diagonal, namely $\Gamma = \mathrm{diag}(\gamma_1, \dots \gamma_{m-p}) > 0$. Regarding the *Annihilator* transfer function denominator $\boldsymbol{\psi}(s)$, it is assumed to be $\boldsymbol{\psi}(s) = s^{\eta+1} + \psi_\eta s^\eta + ... + \psi_1 s + \psi_0$. The only precaution to consider is constraining $\psi_0 = 1$. This is done to keep the *Annihilator* static gain $\Omega_{an} = N_0^{\perp}/\psi_0$ fixed. If this were not the case, the structure of ∇J would change. Instead, by varying Γ, only the gradient descent rate is affected in the *Optimizer*. It is worth pointing out that the properties (e.g., convexity) of (23) are not known a priori, thus its solution is agnostic to the optimization algorithm's choice.

Algorithm 2. **Allocator optimization**

- Design the dynamic *Annihilator* following Algorithm 1;
- Design the steady-state *Optimizer* as in (22), choosing the cost function to be minimized (6) and Γ according to a suitable convergence rate;
- Solve the optimization problem defined in (23), using Γ and $\boldsymbol{\psi}(s)$ previously chosen as the initial condition of the numerical solver;
- Define the robust *Allocator* as the cascade of the *Optimizer* and the *Annihilator* using the optimal value found.

5. NUMERICAL SIMULATION

This section supports the results previously presented through numerical simulations on an example model. More specifically, the plant and controller are taken from Zaccarian (2009) and reported here for completeness. The nominal plant P_0 in (2) is described by the matrices

$$A_0 = \begin{bmatrix} -0.157 & 0.094 \\ -0.416 & 0.45 \end{bmatrix}, \quad B_0 = \begin{bmatrix} 0.87 & 0.253 & 0.743 \\ 0.39 & 0.354 & 0.65 \end{bmatrix}, \qquad (24a)$$

$$C_0 = [0 \ 1], \qquad D_0 = [0 \ 0 \ 0], \qquad (24b)$$

while the controller C in (3) by

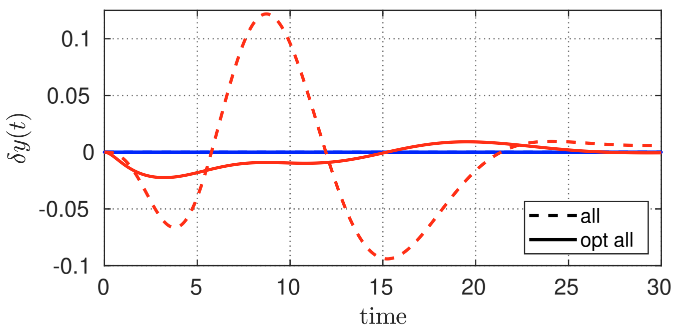

Fig. 4. Output variation $\delta y(t)$ of the closed loop system with a non-optimized *Allocator* (dashed), and with the optimized *Allocator* (solid), with respect to the original closed-loop system; in blue the signals of the nominal plant and in red the signals of a perturbed plant.

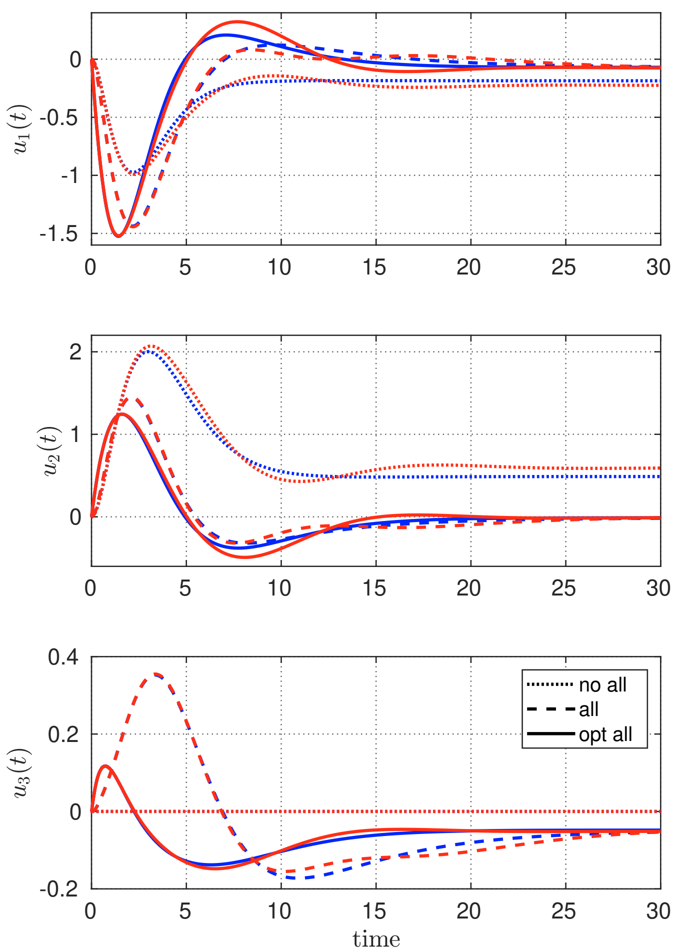

Fig. 5. Control inputs u_i of the closed-loop system without *Allocator* (dotted), with a non-optimized *Allocator* (dashed), and with the optimized *Allocator* (solid); in blue the signals of the nominal plant and in red the signals of a perturbed plant.

$$A_c = \begin{bmatrix} -1.57 & 0.5767 & 0.822 & -0.65 \\ -0.9 & -0.501 & -0.94 & 0.802 \\ 0 & 1 & -1.61 & 1.614 \\ 0 & 0 & 0 & 0 \end{bmatrix}, \quad B_r = \begin{bmatrix} 0 \\ 0 \\ 0 \\ 1 \end{bmatrix} \tag{25a}$$

$$C_c = \begin{bmatrix} 1.81 & -1.2 & -0.46 & 0 \\ -0.62 & 1.47 & 0.89 & 0 \\ 0 & 0 & 0 & 0 \end{bmatrix}, \quad D_r = \begin{bmatrix} 0 \\ 0 \\ 0 \end{bmatrix}, \tag{25b}$$

with $B_c = -B_r$, $D_c = -D_r$, satisfying Assumption 1. The set $\mathcal{P}$ considered has cardinality $|\mathcal{P}| = N = 10$, where each plant $P \in \mathcal{P}$ with $P \neq P_0$ is obtained by perturbing all elements of the nominal plant matrices (A_0, B_0) by 10 percent simultaneously.

As described in Section 3, the input *Allocator* is designed as the cascade of an *Optimizer* and an *Annihilator*. Following Algorithm 1, the dynamic *Annihilator* is calculated based on the nominal plant (24) by choosing a numerator of degree $\eta = n = 2$ and as denominator a Hurwitz polynomial of degree $\eta + 1 = 3$. The structure of the *Optimizer* is defined successively according to the cost function to be minimized, with an initial gain matrix equal to I_{m-p}. The optimization process is performed following Algorithm 2 on the set $\mathcal{P}$. More specifically, linear and nonlinear allocation problems are addressed.

Linear allocation The first simulation focuses on reducing the steady-state Euclidean norm of the plant input u_∞, namely designing an *Allocator* to minimize the quadratic cost function described by

$$J(u_\infty) = \frac{1}{2}\|u_\infty\|^2. \tag{26}$$

This cost function defines a linear allocation problem, since substituting the gradient of (26) in (22) the *Optimizer* dynamics are described by

$$\dot{x}_{op} = -\Gamma\Omega_{an}^{\mathrm{T}}\Omega_{an}x_{op} - \Gamma\Omega_{an}^{\mathrm{T}}y_c, \tag{27a}$$
$$v = x_{op}. \tag{27b}$$

Figs. 4 and 5 show how the non-optimized *Allocator* solves the Problem 1 on the nominal plant but (I) fails on a perturbed one. After the optimization process, the performance on the nominal case is preserved, and the output mismatch is improved on the perturbed case. In particular, Fig. 4 shows that, in the nominal case, the output of the closed-loop system is identical for both the non-optimized and optimized *Allocator*. In contrast, in the perturbed case, the output invisibility is lost. Indeed, a non-negligible mismatch between the allocated and non-allocated trajectories is significantly reduced after optimization. Fig. 5 shows how, in both cases, the *Allocator* modifies the original plant input to converge to the optimal steady-state value minimizing (26).

Nonlinear allocation The second simulation considers the problem of keeping the steady-state value of the plant input u_∞ away from a soft-saturation region, namely designing an *Allocator* to minimize the nonlinear cost function described by

$$J(u_\infty) = \frac{1}{2}\|\mathrm{dz}(u_\infty)\|^2, \tag{28}$$

where $\mathrm{dz}(u_{i,\infty}) = \mathrm{sign}(u_{i,\infty})\max\{0, |u_{i,\infty}| - \bar{u}_i\}$, with $\bar{u}_i$ the i-th saturation amplitude bound. This defines a nonlinear allocation problem, since substituting the gradient of (28) in (22) the *Optimizer* is represented by

$$\dot{x}_{op} = -\Gamma\Omega_{an}^{\mathrm{T}}\mathrm{dz}(y_c + \Omega_{an}x_{op}), \tag{29a}$$
$$v = x_{op}, \tag{29b}$$

Figs. 6 and 7 confirm that the optimized allocator improves the output mismatch while maintaining the optimality of the plant input at steady-state. Hence, the proposed approach is valid even in the nonlinear case.

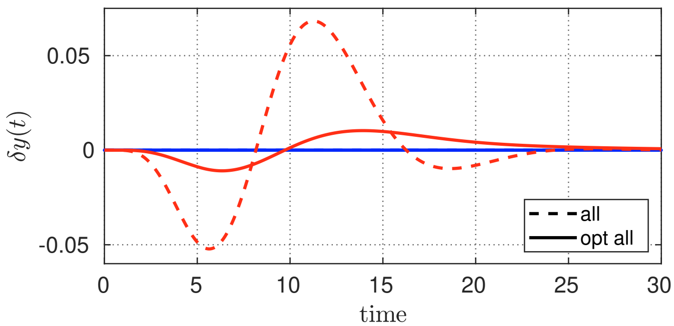

Fig. 6. Output variation $\delta y(t)$ of the closed loop system with a non-optimized *Allocator* (dashed), and with the optimized *Allocator* (solid), with respect to the original closed-loop system; in blue the signals of the nominal plant and in red the signals of a perturbed plant.

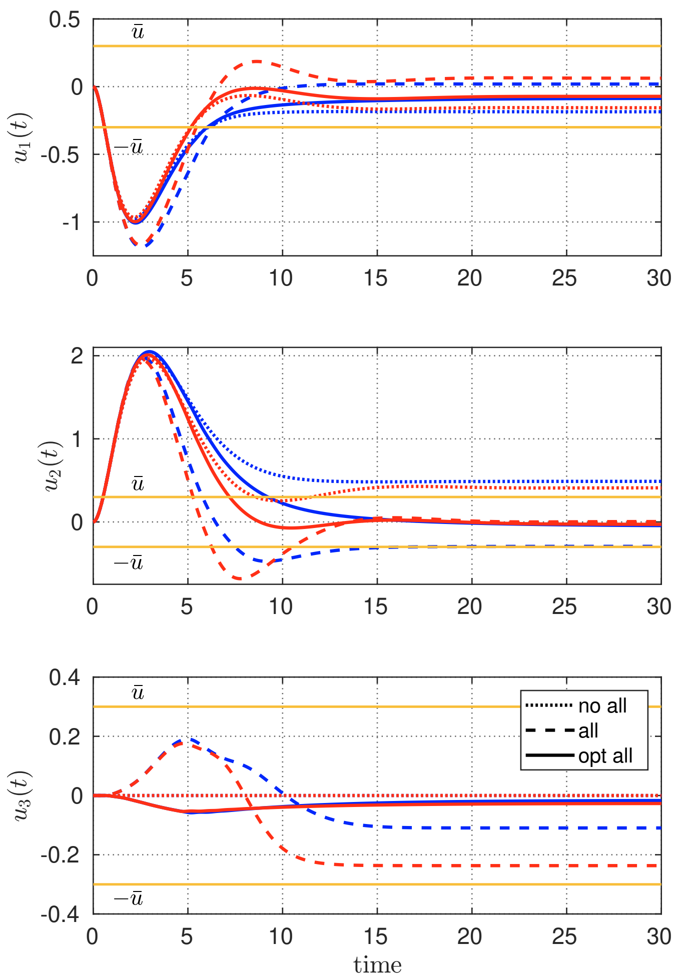

Fig. 7. Control inputs u_i of the closed-loop system without *Allocator* (dotted), with a non-optimized *Allocator* (dashed), and with the optimized *Allocator* (solid); in blue the signals of the nominal plant, in red the signals of a perturbed plant, and in yellow the saturation bounds $\bar{u}$.

6. CONCLUSION

This paper introduces the problem of dynamic input allocation in the presence of plant uncertainties. We provide a procedure to design a robust *Allocator* to address plant uncertainties, applicable for linear and nonlinear *Optimizer* dynamics (22). Such an approach relies on numerical optimization methods to exploit the *Allocator* design parameters. Furthermore, a novel numerical receipt is proposed to design a dynamic *Annihilator* based on polynomial factorization algorithm 1. Numerical simulations confirm the effectiveness of this method, both on linear and nonlinear robust allocation problems. Future developments will consider a relaxation of the constraints in (23) on the *Optimizer* and *Annihilator* dynamics to improve the output invisibility property further.

REFERENCES

Ambrosino, G., DeTommasi, G., et al. (2011). On dynamic input allocation for set-point regulation of the JET tokamak plasma shape. In *IEEE International Conference on Control Applications*, 1315–1320.

Argha, A., Su, S.W., et al. (2019). Static output feedback fault tolerant control using control allocation scheme. *International Journal of Robust and Nonlinear Control*, 29(1), 98–116.

Boncagni, L., Galeani, S., et al. (2011). Plasma position and elongation regulation at FTU using dynamic input allocation. *IEEE Transactions on Control Systems Technology*, 20(3), 641–651.

Cristofaro, A. and Galeani, S. (2014). Output invisible control allocation with steady-state input optimization for weakly redundant plants. In *IEEE Conference on Decision and Control*, 4246–4253.

Esposito, B., Boncagni, L., et al. (2016). Runaway electron generation and control. *Plasma Physics and Controlled Fusion*, 59(1), 014044.

Faddeev, D. and Faddeeva, V. (1981). Computational methods of linear algebra. *Journal of Soviet Mathematics*, 15, 531–650.

Furci, M., Nainer, C., et al. (2019). Input allocation for the propeller-based over-actuated platform ROSPO. *IEEE Transactions on Control Systems Technology*, 28(6), 2720–2727.

Galeani, S. and Pettinari, S. (2014). On dynamic input allocation for fat plants subject to multi-sinusoidal exogenous inputs. In *IEEE Conference on Decision and Control*, 2396–2403.

Galeani, S. and Sassano, M. (2018a). Data-driven dynamic control allocation for uncertain redundant plants. In *IEEE Conference on Decision and Control*, 5494–5499.

Galeani, S. and Sassano, M. (2018b). Output regulation for redundant plants via orthogonal moments. In *IEEE European Control Conference*, 1945–1950.

Galeani, S., Serrani, A., et al. (2015). On input allocation-based regulation for linear over-actuated systems. *Automatica*, 52, 346–354.

Hamandi, M., Usai, F., et al. (2021). Design of multirotor aerial vehicles: A taxonomy based on input allocation. *The International Journal of Robotics Research*, 40(8-9), 1015–1044.

Johansen, T.A. and Fossen, T.I. (2013). Control allocation—a survey. *Automatica*, 49(5), 1087–1103.

Trégouët, J.F., Arzelier, D., et al. (2014). Reaction wheels desaturation using magnetorquers and static input allocation. *IEEE Transactions on Control Systems Technology*, 23(2), 525–539.

Zaccarian, L. (2009). Dynamic allocation for input redundant control systems. *Automatica*, 45(6), 1431–1438.